Environmental Science & Technology

ARTICLE

pubs.acs.org/est

Field Validation of Anaerobic Degradation Pathways for Dichlorodiphenyltrichloroethane (DDT) and 13 Metabolites in Marine Sediment Cores from China

Huan-Yun Yu,[†,§] Lian-Jun Bao,[†,§] Yan Liang,[‡] and Eddy Y. Zeng[*,†]

[†]State Key Laboratory of Organic Geochemistry, Guangzhou Institute of Geochemistry, Chinese Academy of Sciences, Guangzhou 510640, China,

[‡]Department of Biology, Hong Kong Baptist University, Hong Kong SAR, China and

[§]Graduate School, Chinese Academy of Sciences, Beijing 100049, China

Supporting Information

ABSTRACT: Although the production and use of dichlorodiphenyltrichloroethane (DDT), a legacy component of persistent organic pollutants, have been highly restricted worldwide, the environmental fate of DDT has remained a great concern as it is not only ubiquitous and bioaccumulative but can also be degraded to a series of metabolites that may be more hazardous ecologically. The present study, taking advantage of the abundant levels of DDT and its metabolites in a subtropical coastal region of China, investigated into the degradation pathways of DDT in natural coastal sediment. Sediment profiles indicated that degradation of 1,1,1-trichloro-2,2-bis-(*p*-chlorophenyl)ethane (*p,p′*-DDT) to 1,1-dichloro-2,2-bis-(*p*-chlorophenyl)ethane (*p,p′*-DDD) mainly occurred in sediment of the top 20 cm layer. 1,1-dichloro-2,2-bis-(*p*-chlorophenyl)ethylene (*p,p′*-DDE), aerobically transformed from *p,p′*-DDT prior to sedimentation, was likely to degrade to 1-chloro-2,2-bis-(*p*-chlorophenyl)ethylene (*p,p′*-DDMU) which was further converted to 2,2-bis(*p*-chlorophenyl)ethylene (*p,p′*-DDNU). In addition, *p,p′*-DDNU could be transformed to 2,2-bis(*p*-chlorophenyl)ethane (*p,p′*-DDNS) and other high-order metabolites. On the other hand, the conversions of *p,p′*-DDD to *p,p′*-DDMU and 1-chloro-2,2-bis-(*p*-chlorophenyl)ethane (*p,p′*-DDMS) to *p,p′*-DDNU were deemed slow in anaerobic sediment. Therefore, the present study confirmed all the degradation pathways involving reductive dechlorination and *p,p′*-DDE being a more important precursor for *p,p′*-DDMU than *p,p′*-DDD in anaerobic sediment, as proposed previously. On the other hand, the present study suggested that *p,p′*-DDMU instead of *p,p′*-DDMS was more likely the precursor for formation of high-order metabolites. Based on the current assessments, use of (DDD+DDE)/DDTs to indicate whether there is fresh DDT input may lead to large uncertainties if the concentrations of high-order metabolites are not negligible. Similarly, ecological risk assessment associated with DDT should be conducted with consideration of high-order DDT metabolites.

INTRODUCTION

The mechanisms for degradation of dichlorodiphenyltrichloroethane (DDT), a legacy pesticide, have been intensively investigated.[1−5] Wedemeyer[6] proposed the metabolic pathways for DDT in vitro catalyzed by *Aerobacter aerogenes*, that is, 1,1,1-trichloro-2,2-bis-(*p*-chlorophenyl)ethane (*p,p′*-DDT)→1,1-dichloro-2,2-bis-(*p*-chlorophenyl)ethane (*p,p′*-DDD)→1-chloro-2,2-bis-(*p*-chlorophenyl)ethylene (*p,p′*-DDMU)→1-chloro-2,2-bis-(*p*-chlorophenyl)ethane (*p,p′*-DDMS)→2,2-bis(*p*-chlorophenyl)ethylene (*p,p′*-DDNU)→2,2-bis(*p*-chlorophenyl)acetic acid (*p,p′*-DDA)→4,4′-dichlorobenzophenone (*p,p′*-DBP) and *p,p′*-DDT→1,1-dichloro-2,2-bis-(*p*-chlorophenyl)ethylene (*p,p′*-DDE), but *p,p′*-DDE was believed not to degrade under aerobic or anaerobic conditions. Later, Planche et al.[7] demonstrated that *p,p′*-DDE in rodents could be degraded to *p,p′*-DDMU, and further to *p,p′*-DDNU, 2,2-bis(*p*-chlorophenyl)ethanol (*p,p′*-DDOH) and *p,p′*-DDA. In 1998, Quensen et al.[5] confirmed that *p,p′*-DDE could be dechlorinated to *p,p′*-DDMU in a microcosm experiment with marine sediment incubated anaerobically. Aislable et al.[1] also found that *p,p′*-DDD could be converted to *p,p′*-DDMS directly by microbial degradation. Recently, Eggen et al.[4] suggested that both *p,p′*-DDD→*p,p′*-DDMU→*p,p′*-DDMS and *p,p′*-DDD→*p,p′*-DDMS could occur and *p,p′*-DDMS could be degraded continually to other high-order metabolites, and *p,p′*-DDE could be transformed to *p,p′*-DDMU, *p,p′*-DDNU and other high-order metabolites as well.

It should be noted that the results discussed above were mainly derived from laboratory experiments, and differences between laboratory processes and processes occurring under natural conditions have been pointed out previously.[8] In addition, degradation of DDT is controlled by a variety of factors, such

Received: February 24, 2011
Accepted: May 2, 2011
Revised: April 25, 2011
Published: May 19, 2011

dx.doi.org/10.1021/es2006397 | Environ. Sci. Technol. 2011, 45, 5245–5252

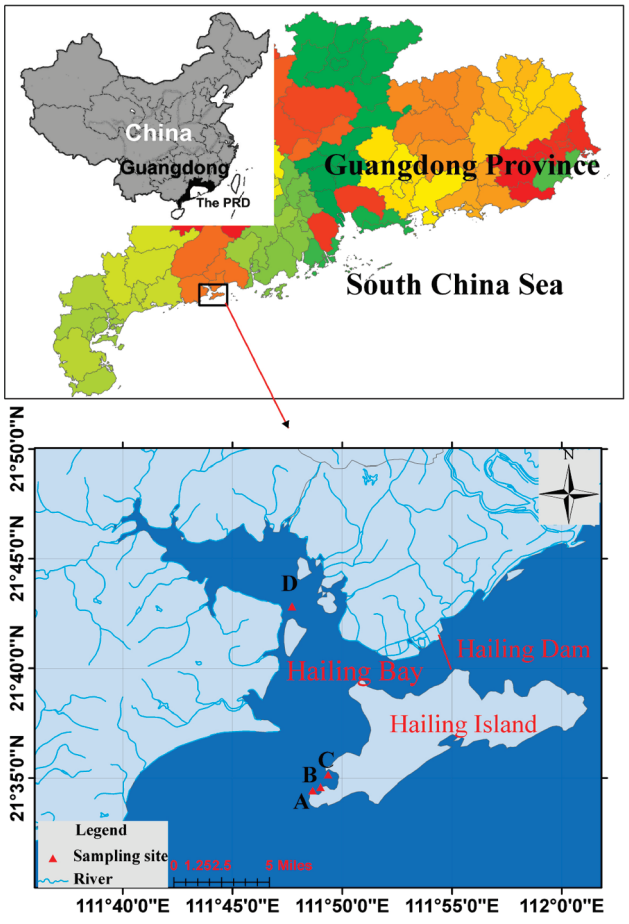

Figure 1. Map showing the general locality of the sampling sites in Hailing Bay of South China. The sediment cores under investigation were collected from A, B, C and D.

as the contents of sulfate and carbon involved, temperature[9] and microbial populations as catalysts.[6] Recently Li et al.[10] found that the transformation of *p,p′*-DDD to *p,p′*-DDMS could occur only with the presence of *S. decolorationis* (an iron-reducing bacterium) and synthetic iron oxide (α-FeOOH). Apparently, further studies of degradation of DDT and its metabolites, especially under field conditions, are necessary for better understanding of the degradation pathways that largely dictate the environmental fate of DDT and its metabolites.

The use of DDT in China began in the early 1950s, and large-scale production and agriculture application of DDT have been forbidden since 1983.[11] However, China's national implementation plan for the Stockholm Convention on persistent organic pollutants revealed that the country still had 3−5 enterprises that produced 3000−4000 tons of technical grade dicofol annually and 19 antifouling paint manufacturers consuming approximately 250 tons/yr of DDT as additives.[12] Previous studies have accredited antifouling paint as a significant source of sediment DDT in harbors and bays of China.[13,14] Our recent investigations[15,16] also found that both sediment and water in a mariculture-supporting bay, Hailing Bay in South China (Figure 1), contained abundant DDXs dominated by *p,p′*-DDD, an anaerobic reductive product of *p,p′*-DDT. These findings have offered the opportunity for further investigations into the degradation pathways of DDT and its metabolites in natural sediments.

Therefore, the present study was undertaken to measure DDT and its metabolites (*o,p′*- and *p,p′*-DDT, -DDD, -DDE, and -DDMS and *p,p′*-DDMU, -DDNU, -DDOH, -DDA, -DDM, and -DBP, 2,2-bis(*p*-chlorophenyl)ethane (*p,p′*-DDNS), sum of which is designated as DDXs) in four sediment cores collected from Hailing Bay, from which degradation pathways of DDT under field conditions were examined. It should be noted that dichlorobenzhydrol (DBH), another metabolite of DDT, was not detected in the present study, because DBH was a major photoproduct of DDT in water phase suggested by previous studies.[17,18] Based on the field data, implications of DDT degradation for source diagnostics and ecological risk assessments are discussed.

MATERIALS AND METHODS

Sample Collection. Sediment core samples were collected from Hailing Bay, located in a subtropical zone of western Guangdong Province in South China (Figure 1) and home to heavy mariculture and tourist activities. The ocean current is interrupted by the Hailing Dam linking the mainland and Hailing Island, resulting in reduced natural dilution of pollutants inside the bay.[19] Sediment cores were collected from sites A, B, C, and D, and collected with a gravity corer (XDB02205; Beijing New Landmark Soil Equipment, Beijing, China) in January 2010 (Supporting Information (SI) Table S1). Sites A, B, and C are adjacent to the Zhapo Town, one of the top 10 fishing harbors in China and capable of accommodating up to 2000 fishing boats.[20] In addition, a large fishing boating maintenance facility is situated at the north bank of the Zhapo Town close to site C. The sediment cores were placed on a specially designed table immediately and sliced in 3 cm increments from top to bottom, resulting in a total of 89 sediment samples. All sliced sediment samples were wrapped with aluminum foil, sealed in polytetrafluoroethylene (PTFE) bags and then transported to the laboratory.

Sample Preparation. All sediment samples were freeze-dried and ground into fine powders. After spiking with surrogate standards, PCB-67 and PCB-191, the samples were Soxhlet extracted with a 1:1 (v:v) acetone and hexane mixture for 48 h, and concentrated to approximately 4 mL with a TurboVap II evaporator (Zymark, Hopkinton, MA). Each extract was divided into two equal portions, for measurements of DDXs and other target analytes, respectively. The portion for DDXs was cleaned with a neutral silica/alumina column and then concentrated to 100 μL under a gentle stream of N_2. Finally, internal standard PCB-82 was added before instrumental analysis. Detailed descriptions of the sediment sample preparation procedures have been given previously.[16,21]

Instrumental Analysis. Concentrations of DDXs excluding *p,p′*-DDA were determined with a Shimadzu model 2010 GC coupled with a Model QP2010 mass spectrometer (MS) (Shimadzu, Japan). The detailed instrumental parameters have been described in our previous study.[22] *p,p′*-DDA was measured with an Agilent liquid chromatography 1200 system equipped with an Agilent 6410 triple quadrupole MS with electrospray ionization in negative mode (Agilent, Palo Alto, CA). Chromatographic separation was achieved on a Zorbax Eclipse plus C18 column (100 × 2.1 mm; particle size 1.8 μm) fitted with a Eclipse Plus C18 Guard column (12.5 × 2.1 mm with a film thickness of 5 um; Agilent). The flow rate was 0.2 mL/min and the mobile phase was ultrapure water containing 0.1% formate (mobile phase A) and methanol (mobile phase B) in a ratio of 10:90. The injection volume was 5 uL, and

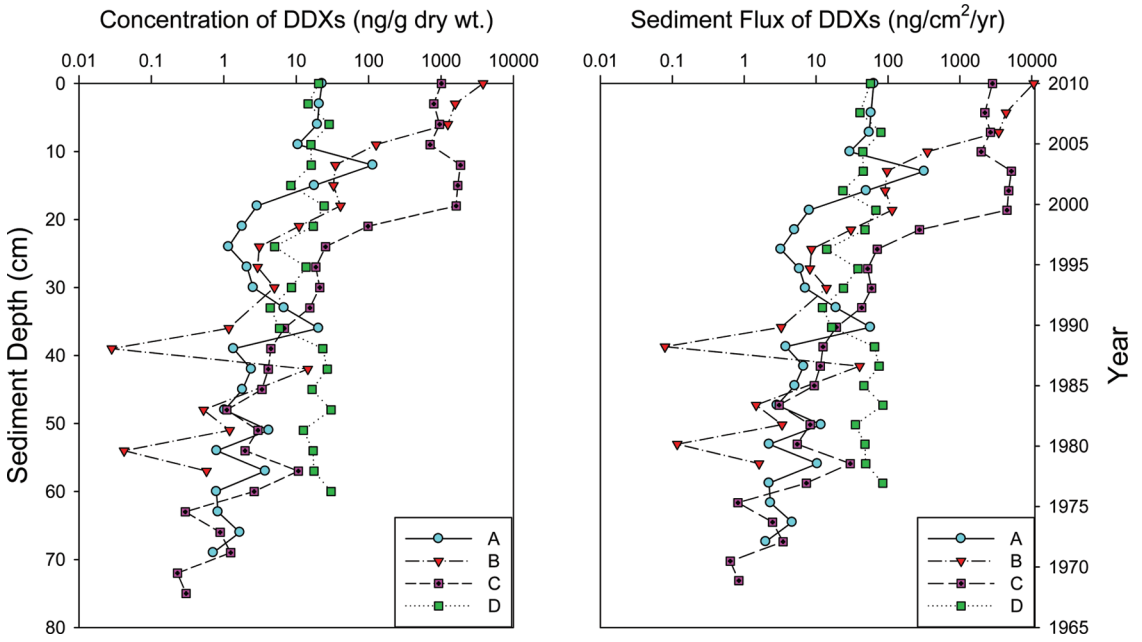

Figure 2. Concentrations and sedimentary fluxes of DDXs (sum of 1,1,1-trichloro-2,2-bis-(*p*-chlorophenyl)ethane (*p*,*p*′-DDT), 2-(*o*-chlorophenyl)-2-(*p*-chlorophenyl)-1,1,1-trichloroethane (*o*,*p*′-DDT), 1,1-dichloro-2,2-bis-(*p*-chlorophenyl)ethane (*p*,*p*′-DDD); 2-(*o*-chlorophenyl)-2-(*p*-chlorophenyl)-1,1-dichloroethane (*o*,*p*′-DDD); 1,1-dichloro-2,2-bis-(*p*-chlorophenyl)ethylene (*p*,*p*′-DDE); 2-(*o*-chlorophenyl)-2-(*p*-chlorophenyl)-1,1- dichloroethylene (*o*,*p*′-DDE); 1-chloro-2,2-bis-(*p*-chlorophenyl)ethane (*p*,*p*′-DDMS); 2-(*o*-chlorophenyl)-2-(*p*-chlorophenyl)-1-chloroethane (*o*,*p*′-DDMS); 1-chloro-2,2-bis-(*p*-chlorophenyl)ethylene (*p*,*p*′-DDMU), 2,2-bis(*p*-chlorophenyl)ethylene (*p*,*p*′-DDNU), 2,2-bis(*p*-chlorophenyl)ethanol (*p*,*p*′-DDOH), 2,2-bis(*p*-chlorophenyl)ethane (*p*,*p*′-DDNS), 2,2-bis(*p*-chlorophenyl)acetic acid (*p*,*p*′-DDA), 2,2-bis(*p*-chlorophenyl)methane (*p*,*p*′-DDM), and 4,4′-dichlorobenzophenone (*p*,*p*′-DBP)) in sediment cores A, B, C, and D collected from an urbanized coastal zone of South China (Figure 1).

the quantifier ion was 235 and qualifier ions were 237 and 239. Nitrogen was used as drying and nebulizing gas. The following optimized source parameters were applied: dry gas flow rate, 10 L/min; drying gas temperature, 300 °C; nebulizing gas pressure, 30 psi; and capillary voltage, +4000/−4000 V. A dwell time of 200 ms, fragmentation voltage of 110 ev, and collision energy of 0 ev were used for data acquisition in the multiple-reaction monitoring mode.

Quantitation Procedures. Concentrations of the target analytes (SI Table S2) except for *p*,*p*′-DDA were determined with an internal calibration method; *p*,*p*′-DDA was quantified with an external calibration procedure. Because no standards were available for *o*,*p*′-/*p*,*p*′-DDMS and *p*,*p*′-DDNS, their concentrations in field samples were estimated based on the response factor of *p*,*p*′-DDD, that is, $C_X = C_{p,p'\text{-DDD}}\, A_X/A_{p,p'\text{-DDD}}$, where C_x and $C_{p,p'\text{-DDD}}$ are the concentrations of the target analyte to be measured (*o*,*p*′-DDMS, *p*,*p*′-DDMS or *p*,*p*′-DDNS) and *p*,*p*′-DDD and A_X and $A_{p,p'\text{-DDD}}$ are the chromatographic areas of the target analyte and *p*,*p*′-DDD. The reporting limit (RL), operationally defined as the lowest concentration of the calibration curve for a specific analyte, was 2 ng/g for 1 g of sediment on a dry weight basis and 1 ng/g for 1 g of antifouling paint on a wet weight basis for individual DDXs (excluding *p*,*p*′-DDA). The reporting limit for *p*,*p*′-DDA was 0.1 ng/g for 1 g of sediment on a dry weight basis.

Sediment Core Dating. The ^{210}Pb activities in sediment subsamples were determined from α radioactivity of ^{210}Pb's decay product ^{210}Po. ^{209}Po, used as a yield monitor and tracer, was measured with computerized multichannel α spectrometry with gold−silicon surface barrier detectors. The excess amounts of ^{210}Po were calculated by subtracting ^{210}Po background activity (^{226}Ra-supported) from total activity, from which the average sedimentation rate of 1.86 cm/yr was obtained using the constant initial ^{210}Pb concentration model.[23]

Quality Assurance/Quality Control. For each batch of 20 field samples, a field blank, a procedural blank, a spiked blank, and a matrix spiked sample and a matrix spiked sample duplicate were also analyzed. The recoveries of the target compounds ranged from 41−68% with relative standard deviations 17% in spiked matrix samples and from 50−78% with relative standard deviations 18% in spiked blank samples. The recoveries of the surrogate standards in all samples were 79 ± 31% for PCB-67 and 68 ± 25% for PCB-191, respectively. Blank values were not subtracted out for all the samples because the concentrations in the procedural and field blank samples were close to or lower than the reporting limits. In addition, during instrumental analysis, a standard solution of *p*,*p*′-DDT was analyzed once for every batch of 10 samples prior to instrumental analysis to ensure the degradation rate of *p*,*p*′-DDT was less than 20%.

Data Analysis. Principal component analysis (PCA) and cluster analysis with a classified method of hierachical cluster using SPSS version 13.0 were used to examine the pathways of DDT metabolism in sediment. In these analyses, only concentrations higher than the reporting limits were used. In addition, the sedimentary flux (F_{sed}; ng/cm^2/yr) of an analyte was estimated with $F_{sed} = Cd\gamma$ where C is the analyte concentration in sediment (ng/g dry wt), d is the sediment density (1.5 g/cm^3), γ is the average sedimentation rate (1.86 cm/yr from ^{210}Pb activity measurements). The water content of sediment does need to be considered in the sedimentary flux estimation because the analyte concentration in sediment and the sediment density are all based on dry weight.

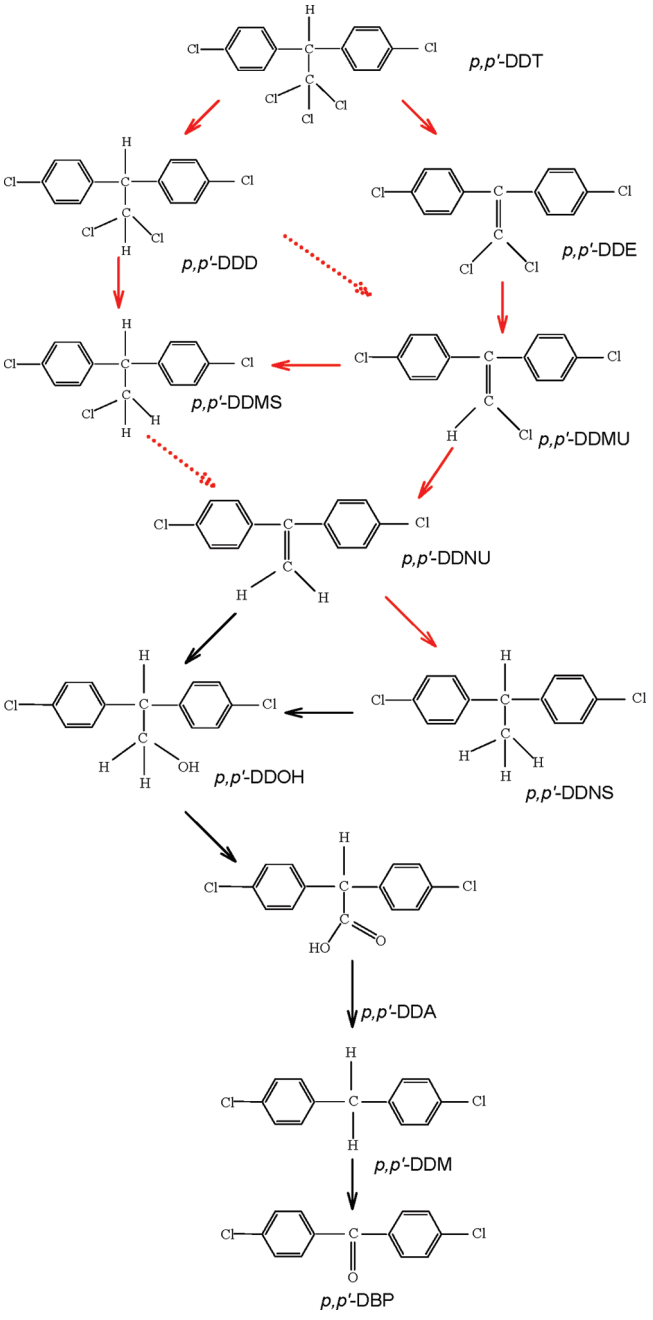

Figure 3. Proposed degradation pathways of 1,1,1-trichloro-2,2-bis-(*p*-chlorophenyl)ethane (*p*,*p*′-DDT), modified from Eggen and Majcherczyk,[4] in sediment of an urbanized coastal zone of South China (Figure 1). The solid red lines indicate the degradation pathways that have been confirmed in the present study and the dotted red lines suggest that the pathways are deemed slow based on the results of the present study. The pathways described with the black solid lines are neither confirmed nor refuted by the present study because of insufficient data.

RESULTS AND DISCUSSION

Occurrence of Target Compounds. Detected target compounds include p,p′-DDT, *o*,*p*′-DDT, *p*,*p*′-DDD, *o*,*p*′-DDD, *p*,*p*′-DDE, *o*,*p*′-DDE, *p*,*p*′-DDMS, *o*,*p*′-DDMS, *p*,*p*′-DDMU, *p*,*p*′-DDNU, *p*,*p*′-DDOH, *p*,*p*′-DDNS, *p*,*p*′-DDA, *p*,*p*′-DDM, *p*,*p*′-DBP, with the detection rates varying between 6.7% and 96% (Figure S1 of the SI) in 89 sediment core samples. *p*,*p*′-DDD was the most frequently detected component (in 96% of the samples), followed by *o*,*p*′-DDT (83%), *p*,*p*′-DDT (80%) and *p*,*p*′-DDNU (80%). Conversely, *p*,*p*′-DDOH (6.7%), *p*,*p*′-DDA (18%) and *p*,*p*′-DDM (22%) were detected in the least numbers of samples. Concentration data (SI Tables S3−S6) show that the target compounds were generally more abundant in cores B and C than in cores A and D. This result appeared to be consistent with the fact that sampling site C is close to the boat maintenance facility, while site B is located at the northern side of a semiopen bay (Figure 1), an ideal sedimentation zone that possibly receives large amounts of suspended materials from the neighboring bay strongly impacted by the boat maintenance facility. On the other hand, sites A and D are in the areas subject to strong tides that substantially weaken net sediment deposition. This notion seems to be supported by another feature in the data (SI Tables S3−S6), that is, the most abundant components was *p*,*p*′-DDD in cores B and C, but was *p*,*p*′-DDT in cores A and D. Apparently, better depositional conditions at sites B and C may have allowed *p*,*p*′-DDT to degrade (more favorably to *p*,*p*′-DDD as will be discussed later) with a larger extent compared to those at A and D.

Sediment Profiles and Depositional Fluxes. The concentration profiles of DDXs showed a decreasing trend with increasing sediment depth in sediment cores B and C (Figure 2a), resulting in also decreasing sedimentary fluxes of DDXs (Figure 2b). This was opposite to the results of Heim et al.[17] and suggested that the area has been receiving newly discharged DDT. It is apparently that the inputs of DDT-containing materials to the coastal sediment has accelerated since the mid 1990s and appeared to become steady at sampling location C. On the other hand, the trend has remained upward at B. Therefore, it may be premature to claim the overall input of DDT residues has peaked, given the limited number of sediment cores examined. As also observed previously, there were substantial differences in abundances and sedimentary fluxes between sediment core B (and C) and A (and D). In addition, there was no systematic pattern associated with the sediment profiles of DDXs at A and D. This simply supported the above-mentioned notion that the sedimentation conditions have been considerably better at B and C than at A and D. It is also interesting to note that both concentrations and fluxes of DDXs dropped to similar levels at all sampling sites prior to 1990 (Figure 2), which may have reflected either the then background level or the net result of downward movement along the sediment column.

Degradation Pathways of DDT in Coastal Sediment. The detection of a large number of abundant DDT metabolites in the sediment core samples (SI Tables S3−S6) has provided a rare opportunity to examine the degradation pathways of DDT in natural sediment, adding to the current knowledge base of the environmental fate of DDT[3−5,17] Based on the information acquired in the present study and the results from a previous study,[4] we propose the following pathways for degradation of *p*,*p*′-DDT and its metabolites in the coastal sediment under investigation (Figure 3): (1) *p*,*p*′-DDT was degraded to *p*,*p*′-DDE under aerobic condition prior to sedimentation, but was reductively transformed to *p*,*p*′-DDD in sediment (after sedimentation) where anaerobic conditions were presumably prevailing; (2) *p*,*p*′-DDD was further converted to *p*,*p*′-DDMS whereas *p*,*p*′-DDE was transformed to *p*,*p*′-DDMU; (3) *p*,*p*′-DDMU was degraded to *p*,*p*′-DDNU which in turn was degraded to both *p*,*p*′-DDOH and *p*,*p*′-DDNS and other high-order metabolites; (4) *p*,

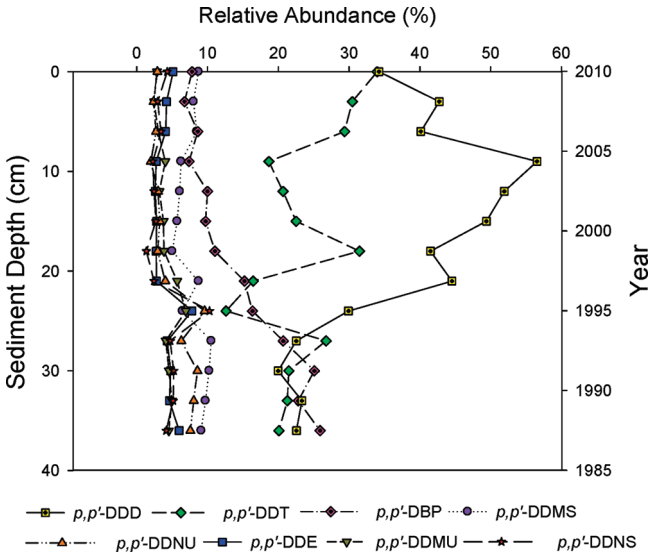

Figure 4. Relative abundances of individual congeners normalized to *p,p′*-DDXs (sum of 1,1,1-trichloro-2,2-bis-(*p*-chlorophenyl)ethane (*p,p′*-DDT), 1,1-dichloro-2,2-bis-(*p*-chlorophenyl)ethane (*p,p′*-DDD), 1,1-dichloro-2,2-bis-(*p*-chlorophenyl)ethylene (*p,p′*-DDE), 1-chloro-2,2-bis-(*p*-chlorophenyl)ethane (*p,p′*-DDMS), 2,2-bis-(*p*-chlorophenyl) ethylene (*p,p′*-DDMU), 2,2-bis(*p*-chlorophenyl)ethylene (*p,p′*-DDNU), 2,2-bis(*p*-chlorophenyl)ethane (*p,p′*-DDNS), and 4,4′-dichlorobenzophenone (*p,p′*-DBP)) in sediment core C (Figure 1).

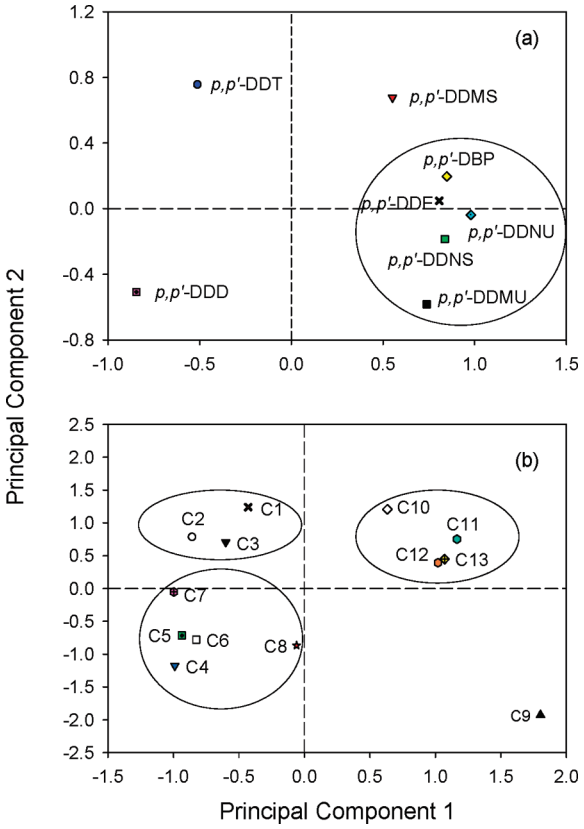

Figure 5. Loading plots for relative abundances of individual congeners normalized to *p,p′*-DDXs (sum of 1,1,1-trichloro-2,2-bis-(*p*-chlorophenyl)ethane (*p,p′*-DDT), 1,1-dichloro-2,2-bis-(*p*-chlorophenyl)ethane (*p,p′*-DDD), 1,1-dichloro-2,2-bis- (*p*-chlorophenyl)ethylene (*p,p′*-DDE), 1-chloro-2,2-bis-(*p*-chlorophenyl)ethane (*p,p′*-DDMS), 2,2-bis-(*p*-chlorophenyl)ethylene (*p,p′*-DDMU), 2,2-bis(*p*-chlorophenyl) ethylene (*p,p′*-DDNU), 2,2-bis(*p*-chlorophenyl)ethane (*p,p′*-DDNS), and 4,4′-dichlorobenzophenone (*p,p′*-DBP)) in sediment core C (SI Figure S1) based on principal component (PC) analysis: distribution of (a) loadings (b) scores (The sediment cores were sliced in 3 cm increments from top to bottom, and C1 is for 0−3 cm, C2 for 3−6 cm, C3 for 6−9 cm, C4 for 9−12 cm, C5 for 12−15 cm, C6 for 15−18 cm, C7 for 18−21 cm, C8 for 21−24 cm, C9 for 24−27 cm, C10 for 27−30 cm, C11 for 30−33 cm, C12 for 33−36 cm, and C13 for 36−39 cm sediment layer). Principal component 1 (PC1) and principal component 2 (PC2) explain 62% and 21% of the overall variance, respectively.

p′-DDMS might not be decomposed easily and transformation rate of *p,p′*-DDD to *p,p′*-DDMU was also deemed slow, which were indicated by the dotted red lines in Figure 3. These proposed degradation pathways are corroborated further with the following observations. In the present study, *p,p′*-DDOH, *p,p′*-DDM and *p,p′*-DDA will not be examined because of their low detection rates (SI Figure S1). In addition, no clear trend was found for the relative abundances of the selected analytes in sediment cores A, B, and D (SI Figures S2−S3), mainly due to low concentration levels of the target compounds, not being long enough or bad sedimentation conditions for these cores. The sediment core from site C (Figure 1), which is 82 cm long and contains relatively high concentrations of the target analytes compared to the other cores (SI Table S5), will be used for the analyses.

Figure 4 displays the relative abundances of the selected analytes throughout the sediment core C. The relative abundances of *p,p′*-DDT and *p,p′*-DDD varied substantially and in opposite directions with increasing sediment depth within the top sediment layer of 25 cm (representing ∼10 yeas of deposition), suggesting that *p,p′*-DDT degraded rapidly to *p,p′*-DDD mainly within the 10 years of deposition. Below the 25 cm depth, the relative abundances of *p,p′*-DDT and *p,p′*-DDD each remained stable at approximately 20−25%. However, *p,p′*-DBP increased from approximately 17−28% between 20 and 35 cm. This result indicated that the secondary or higher-order metabolites of *p,p′*-DDT predominantly degraded in sediment of sub-25 cm layer. In addition, the relative abundance of *p,p′*-DBP increased continuously throughout the sediment depths, pointing to the likelihood of *p,p′*-DBP as the main end product of *p,p′*-DDT. The high relative abundances of *p,p′*-DDD (20−56%; Figure 4) suggested that DDD was the major degradation product of DDT under anaerobic conditions, similar to the results reported previously.[1,24] Furthermore, *p,p′*-DDE, *p,p′*-DDMU, *p,p′*-DDNU, and *p,p′*-DDNS peaked around 1995 where the relative abundance of *p,p′*-DDT reached the lowest value, corroborating the likelihood for transformation of *p,p′*-DDT into *p,p′*-DDE, *p,p′*-DDMU, *p,p′*-DDNU and *p,p′*-DDNS. On the other hand, the relative abundance of *p,p′*-DDMS did not show such a pattern, probably indicating that it may undergo a different degradation pathway compared to other metabolites.

Further evidence for the proposed degradation pathways can be derived from the PCA results (Figure 5). For example, PC 1 had high positive loadings of *p,p′*-DDE, *p,p′*-DDMU, *p,p′*-DDNU, *p,p′*-DDNS, and *p,p′*-DBP (Figure 5a), suggesting they were closely related in terms of degradation pathways. PC 1 also had a high negative loading of *p,p′*-DDD, probably indicating no significant correlation of *p,p′*-DDD with the above-mentioned metabolites (i.e., *p,p′*-DDE, *p,p′*-DDMU, *p,p′*-DDNU, *p,p′*-DDNS,

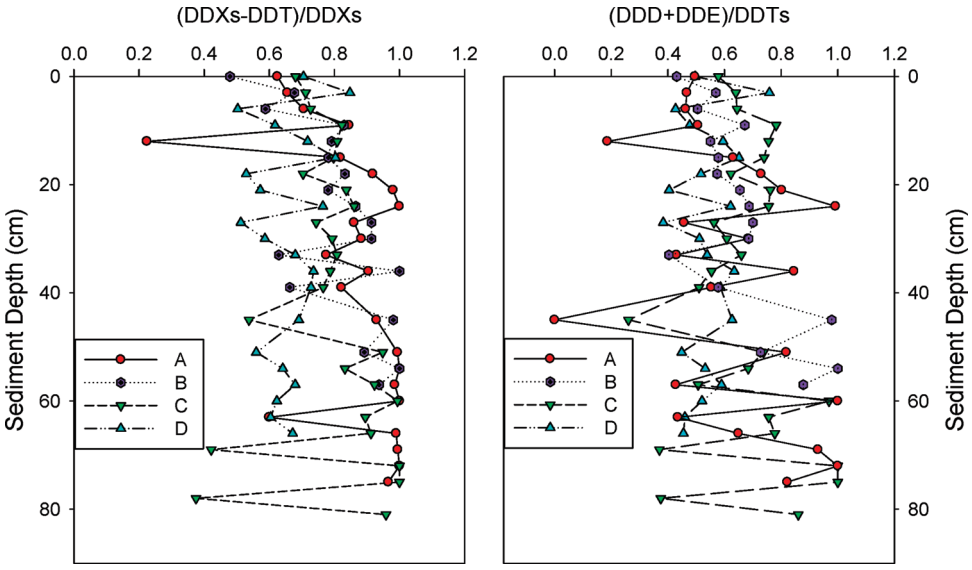

Figure 6. Values of (DDD+DDE)/DDTs and (DDXs−DDT)/ DDXs in 89 sediment core samples. DDD: sum of 1,1-dichloro-2,2-bis-(*p*-chlorophenyl)ethane (*p,p′*-DDD) and 2-(*o*-chlorophenyl)-2-(*p*-chlorophenyl)-1,1-dichloroethane (*o,p′*-DDD); DDE: sum of 1,1-dichloro-2,2-bis-(*p*-chlorophenyl)ethylene (*p,p′*-DDE) and 2-(*o*-chlorophenyl)-2-(*p*-chlorophenyl)-1,1- dichloroethylene (*o,p′*-DDE); DDTs: sum of 1,1,1-trichloro-2,2-bis-(*p*-chlorophenyl)ethane (*p,p′*-DDT) and 2-(*o*-chlorophenyl)-2-(*p*-chlorophenyl)-1,1,1-trichloroethane (*o,p′*-DDT), *o,p′* and *p,p′*-DDD and -DDE; DDXs: sum of *o,p′* and *p,p′*-DDT, -DDD, -DDE, and 1-chloro-2,2-bis-(*p*-chlorophenyl)ethane (*p,p′*-DDMS), 2-(*o*-chlorophenyl)-2-(*p*-chlorophenyl)-1-chloroethane (*o,p′*-DDMS), 1-chloro-2,2-bis-(*p*-chlorophenyl)ethylene (*p,p′*-DDMU), 2,2-bis(*p*-chlorophenyl)ethylene (*p,p′*-DDNU), 2,2-bis(*p*-chlorophenyl)ethanol (*p,p′*-DDOH), 2,2-bis(*p*-chlorophenyl)ethane (*p,p′*-DDNS), 2,2-bis(*p*-chlorophenyl)acetic acid (*p,p′*-DDA), 2,2-bis(*p*-chlorophenyl)methane (*p,p′*-DDM), and 4,4′-dichlorobenzophenone (*p,p′*-DBP); DDT: sum of *o,p′* and *p,p′*-DDT.

and *p,p′*-DBP). In addition, PC 1 and PC 2 had high loadings of *p,p′*-DDMS (Figure 5a), that is, *p,p′*-DDMS might somewhat correlate with all other metabolites. Similar to *p,p′*-DDMS, PC 1 and PC 2 also had high negative and positive loadings of *p,p′*-DDT, respectively. Based on the sample scores (Figure 5b), the sediment samples can be divided into three groups: C1, C2, and C3 in the upper layer and closely correlated to *p,p′*-DDT; C4, C5, C6, C7, and C8 in the middle layer and highly associated with *p,p′*-DDD; and C10, C11, C12, and C13 in the deeper layer with close relationship with *p,p′*-DDE, *p,p′*-DDMU, *p,p′*-DDNU, *p,p′*-DDNS, and *p,p′*-DBP. These groupings, combined with the observations from Figure 5a, pointed to different degradation phases for *p,p′*-DDT and its metabolites during different sedimentary periods, consistent with the above-mentioned conclusion that the conversion of *p,p′*-DDT to *p,p′*-DDD mainly occurred in the top 25 cm sediment layer while degradation of secondary or high-order metabolites of *p,p′*-DDT predominantly proceeded in the sub-25 cm layer. The results from cluster analysis (SI Figure S4) also showed that all metabolites can be divided into four groups, that is, *p,p′*-DDT, *p,p′*-DDD, *p,p′*-DDMS, and sum of all other metabolites (*p,p′*-DDE, *p,p′*-DDMU, *p,p′*-DDNU, and *p,p′*-DDNS).

Overall, the results of the present study provided field evidence for the degradation pathways of *p,p′*-DDT→*p,p′*-DDD→*p,p′*-DDMS and *p,p′*-DDE→*p,p′*-DDMU→*p,p′*-DDNU (solid red lines in Figure 3), suggested by previous studies.[1,4] All these transformations involve reductive dechlorination and have been ratified as the predominant mechanism for DDT transformation under anaerobic conditions.[10] Besides, the present study also favored the degradation pathways of *p,p′*-DDMU to *p,p′*-DDMS and *p,p′*-DDNU to *p,p′*-DDNS through reductive hydrogenation (solid red lines in Figure 3), which have been demonstrated by previous studies.[6,25] Wedemeyer[6] proposed that *p,p′*-DDD and *p,p′*-DDMS can be dehydrochlorinated to *p,p′*-DDMU and *p,p′*-DDNU by microorganisms, respectively, under anaerobic conditions. On the other hand, these transformations (indicated by dotted red lines in Figure 3) were deemed slow in the sediment sampled in the present study. In addition, the results of the present study were different from the degradation pathways for anaerobic transformation of *p,p′*-DDT by bacteria,[1] that is, high-order metabolites such as *p,p′*-DDNU, -DDOH, -DDA, -DDM and -DBP were derived mainly from the degradation of *p,p′*-DDMS. Our study, on the other hand, demonstrated that *p,p′*-DDMU was a more important precursor for formation of high-order metabolites. Apparently, transformation of DDT may be a complex and site-specific process under field conditions and still requires additional investigations.

Implications for Source Diagnostics and Ecological Risk Assessment. The value of (DDD+DDE)/DDTs (DDD is defined as the sum of *o,p′* and *p,p′*-DDD and DDE is the sum of *o,p′* and *p,p′*-DDE) is often used to indicate whether fresh input of DDT is prevailing.[26,27] However, the values of (DDD+DDE)/DDTs were all lower than those of (DDXs−DDT)/DDXs (DDT is defined as the sum of *o,p′* and *p,p′*-DDT) in the sediment core samples (SI Figure S5), attributable to the occurrence of other metabolites in addition to DDD and DDE. Apparently, use of (DDD+DDE)/DDTs would undermine source diagnostics if the concentrations of higher-order metabolites are not negligible. Besides, it should be noted that extremely slow degradation rate of DDT is a prerequisite for using (DDD+DDE)/DDTs to determine whether fresh input of DDT is present.[28] Our previous study[16] found that the relative abundances of *p,p′*-DDD were all higher than or comparable to those of *p,p′*-DDT in both surface sediment and water samples collected from the same general area sampled in the present study, indicating that transformation rate of DDT in the study

region may not be sufficiently slow after all to meet the criterion for the proper use of (DDD+DDE)/DDTs. It concluded that historical residues remained the main source of DDTs in Hailing Bay, based on the values of (DDD+DDE)/DDTs.[16] Clearly, this conclusion may need to be re-examined. The values of (DDXs−DDT)/DDXs showed an increasing trend with increasing sediment depth (Figure 6), indicating gradual degradation of DDT with time. This trend for the values of (DDD+DDE)/DDTs can be found only in the top 25 cm sediment layer and is not significant in the sub-25 cm layer (Figure 6), consistent with the conclusion that high-order metabolites of *p,p′*-DDT predominantly proceeded in the sub-25 cm layer mentioned in the preceding section. Therefore, the disappearance of the increasing trend for (DDD+DDE)/DDTs in the sub-25 cm layer could be attributable to the formation of other metabolites of DDT in addition to DDD and DDE.

Another implication from the results presented herein is concerning the assessment of ecological risk with DDT, which has long been conducted without accounting for the high-order metabolites such as *p,p′*-DDMU, -DDMS, -DDNU, -DDNS, and -DBP. Limited data have suggested that the toxicities of high-order metabolites of DDT may be more potent than DDT and its secondary metabolites. For example, Megharaj et al.[29] found that the apparent toxicity of DDT and its metabolites to soil algae followed the order of *p,p′*-DDT < *p,p′*-DDE < *p,p′*-DDMU< *p,p′*-DDOH < *p,p′*-DDA < *p,p′*-DDD < *p,p′*-DBP. Besides, *p,p′*-DDOH was the most effective component among the DDT metabolites at inhibiting progesterone-induced β-galactosidase activity.[30] In the present study, the sediment samples from the top 36 cm layer at site C contained a large number of the target analytes with the relative abundances of the sum of high-order metabolites in the range of 19−52%. This result clearly demonstrated that nontarget screening analysis may often be needed for better assessment of the ecological risk levels imposed by DDT and its metabolites. On the other hand, the ecological toxic effects of high-order DDT metabolites have remained largely unknown; therefore, additional toxicological studies are deemed necessary and important.

■ ASSOCIATED CONTENT

Ⓢ Supporting Information. Additional tables and figures containing information about field sampling, target analytes, detection frequency of the target analytes and cluster analysis. This material is available free of charge via the Internet at http://pubs.acs.org.

■ AUTHOR INFORMATION

Corresponding Author

*Phone: 86-20-85291421; fax: 86-20-85290706; e-mail: eddyzeng@gig.ac.cn.

■ ACKNOWLEDGMENT

The present study was financially supported by the Natural Science Foundation of Guangdong Province (No. 9251064-004000002), the Ministry of Science and Technology of China (No. 2007AA06Z410), and the National Natural Science Foundation of China (No. 40821003). We are also grateful to Ru-Lang Shen, Bao-Zhong Zhang, Yan-Li Wei, Kai Zhang and Ye-Tian Li for sample collection and Xiao-Min Lin for laboratory support. This is contribution No. IS-1337 from GIGCAS.

■ REFERENCES

(1) Aislabie, J. M.; Richards, N. K.; Boul, H. L. Microbial degradation of DDT and its residues—A review. *N. Z. J. Agric. Res.* **1997**, *40* (2), 269–282.

(2) Huang, H. J.; Liu, S. M.; Kuo, C. E. Anaerobic biodegradation of DDT residues (DDT, DDD, and DDE) in estuarine sediment. *J. Environ. Sci. Health, Part B* **2001**, *36* (3), 273–288.

(3) Sayles, G. D.; You, G. R.; Wang, M. X.; Kupferle, M. J. DDT, DDD, and DDE dechlorination by zero-valent iron. *Environ. Sci. Technol.* **1997**, *31* (12), 3448–3454.

(4) Eggen, T.; Majcherczyk, A. Effects of zero-valent iron (Fe^0) and temperature on the transformation of DDT and its metabolites in lake sediment. *Chemosphere* **2006**, *62* (7), 1116–1125.

(5) Quensen, J. F.; Mueller, S. A.; Jain, M. K.; Tiedje, J. M. Reductive dechlorination of DDE to DDMU in marine sediment microcosms. *Science* **1998**, *280* (5364), 722–724.

(6) Wedemeyer, G. Dechlorination of 1,1,1-trichloro-2,2-bis (*p*-chloro-phenyl) ethane by aerobacter aerogenes I. metabolic products. *Appl. Microbiol.* **1967**, *15* (3), 569–&.

(7) Planche, G.; Croisy, A.; Malaveille, C.; Tomatis, L.; Bartsch, H. Metabolic and mutagenicity studies on DDT and 15 derivatives - Detection of 1,1-bis(para-chlorophenyl)-2,2-dichloroethane and 1,1-bis(para-chlorophenyl)-2,2,2-trichloroethyl acetate (kelthane acetate) as mutagens in salmonella-typhimurium and of 1,1-bis(para-chlorophenyl) ethylene-oxide, a likely metabolite, as an akylating agenti. *Chem.-Biol. Interact.* **1979**, *25* (2−3), 157–175.

(8) Renner, R. "Natural" remediation of DDT, PCBs debated. *Environ. Sci. Technol.* **1998**, *32* (15), 360A–363A.

(9) Quensen, J. F.; Tiedje, J. M.; Jain, M. K.; Mueller, S. A. Factors controlling the rate of DDE dechlorination to DDMU in Palos Verdes margin under anaerobic conditions. *Environ. Sci. Technol.* **2001**, *35* (2), 286–291.

(10) Li, F. B.; Li, X. M.; Zhou, S. G.; Zhuang, L.; Cao, F.; Huang, D. Y.; Xu, W.; Liu, T. X.; Feng, C. H. Enhanced reductive dechlorination of DDT in an anaerobic system of dissimilatory iron-reducing bacteria and iron oxide. *Environ. Pollut.* **2010**, *158* (5), 1733–1740.

(11) United Nations Development Programme (UNDP). China-Improvement of DDT-based production of dicofol and introduction of alternative technologies including IPM for leaf mites control in China. http://www.thegef.org/gef/sites/thegef.org/files/repository/China_09-08-08_Improvement_DDT-based_production_Dicofol_IPM.pdf (accessed April 2011).

(12) The People's Republic of China. National Implementation Plan for the Stockholm Convention on Persistent Organic Pollutants. http://www.pops.int/documents/implementation/nips/submissions/China_NIP_En.pdf (accessed April 2011).

(13) Lin, T.; Hu, Z. H.; Zhang, G.; Li, X. D.; Xu, W. H.; Tang, J. H.; Li, J. Levels and mass burden of DDTs in sediments from fishing harbors: The importance of DDT-containing antifouling paint to the coastal environment of China. *Environ. Sci. Technol.* **2009**, *43* (21), 8033–8038.

(14) Wang, J.; Guo, L. L.; Li, J.; Zhang, G.; Lee, C. S. L.; Li, X. D.; Jones, K. C.; Xiang, Y. R.; Zhong, L. J. Passive air sampling of DDT, chlordane and HCB in the Pearl River Delta, South China: Implications to regional sources. *J. Environ. Monit.* **2007**, *9* (6), 582–588.

(15) Xing, Y. N.; Guo, Y.; Xie, M.; Shen, R. L.; Zeng, E. Y. Detection of DDT and its metabolites in two estuaries of South China using a SPME-based device: First report of *p,p′*-DDMU in water column. *Environ. Pollut.* **2009**, *157* (4), 1382–1387.

(16) Yu, H.-Y.; Guo, Y.; Bao, L.-J.; Zeng, E. Y. Persistent halogenated compounds in two typical marine aquaculture zones of South China. *Mar. Pollut. Bull.* (in press).

(17) Heim, S.; Ricking, M.; Schwarzbauer, J.; Littke, R. Halogenated compounds in a dated sediment core of the Teltow canal, Berlin: Time

related sediment contamination. *Chemosphere* **2005**, *61* (10), 1427–1438.

(18) Llompart, M.; Lores, M.; Lourido, M.; Sanchez-Prado, L.; Cela, R. On-fiber photodegradation after solid-phase microextraction of *p,p′*-DDT and two of its major photoproducts, *p,p′*-DDE and *p,p′*-DDD. *J. Chromatogr., A* **2003**, *985* (1−2), 175–183.

(19) Qiu, Y.-W.; Zhu, L.-S.; Xu, M.-C. C.; Xiu-Hua The characteristics of key environmental factors in the water of Hailing Bay, Guangdong Province. *Mar. Sci.* **2006**, *30* (4), 20–24.

(20) 51766.com. Fishing festival of South China Sea-fishing boat in Zhapo fishing harbor. http://www.51766.com/xinwen/11003/1100385005.html (accessed April 2011).

(21) Zhang, B.-Z.; Yu, H.-Y.; You, J.; Zeng, E. Y. Input pathways of organochlorine pesticides to typical freshwater cultured fish ponds of South China: Hints for pollution control. *Environ. Toxicol. Chem.* **2011**, *30* (6), 1272−1277.

(22) Meng, X.-Z.; Zeng, E. Y.; Yu, L.-P.; Mai, B.-X.; Luo, X.-J.; Ran, Y. Persistent halogenated hydrocarbons in consumer fish of China: Regional and global implications for human exposure. *Environ. Sci. Technol.* **2007**, *41* (6), 1821–1827.

(23) Zhang, G.; Parker, A.; House, A.; Mai, B. X.; Li, X. D.; Kang, Y. H.; Wang, Z. S. Sedimentary records of DDT and HCH in the Pearl River Delta, South China. *Environ. Sci. Technol.* **2002**, *36* (17), 3671–3677.

(24) Yim, Y. J.; Seo, J.; Kang, S. I.; Ahn, J. H.; Hur, H. G. Reductive dechlorination of methoxychlor and DDT by human intestinal bacterium Eubacterium limosum under anaerobic conditions. *Arch. Environ. Contam. Toxicol.* **2008**, *54* (3), 406–411.

(25) Lal, R.; Saxena, D. M. Accumulation, metabolism, and effects of organochlorine insecticides on microorganisms. *Microbiol. Rev.* **1982**, *46* (1), 95–127.

(26) Doong, R. A.; Sun, Y. C.; Liao, P. L.; Peng, C. K.; Wu, S. C. Distribution and fate of organochlorine pesticide residues in sediments from the selected rivers in Taiwan. *Chemosphere* **2002**, *48* (2), 237–246.

(27) Zhou, R. B.; Zhu, L. Z.; Yang, K.; Chen, Y. Y. Distribution of organochlorine pesticides in surface water and sediments from Qiantang River, East China. *J. Hazard. Mater.* **2006**, *137* (1), 68–75.

(28) Hitch, R. K.; Day, H. R. Unusual persistence of DDT in some western USA soils. *Bull. Environ. Contam. Toxicol.* **1992**, *48* (2), 259–264.

(29) Megharaj, M.; Boul, H. L.; Thiele, J. H. Effects of DDT and its metabolites on soil algae and enzymatic activity. *Biol. Fertil. Soils* **1999**, *29* (2), 130–134.

(30) Klotz, D. M.; Ladlie, B. L.; Vonier, P. M.; McLachlan, J. A.; Arnold, S. F. *O,p′*-DDT and its metabolites inhibit progesterone-dependent responses in yeast and human cells. *Mol. Cell. Endocrinol.* **1997**, *129* (1), 63–71.